Bifurcations of the Atlantic thermohaline circulation in response to changes in the hydrological cycle

Stefan Rahmstorf

Institut für Meereskunde, Düsternbrooker Weg 20, 24105 Kiel, Germany

The sensitivity of the North Atlantic thermohaline circulation to the input of fresh water is studied using a global ocean circulation model coupled to a simplified model atmosphere. Owing to the nonlinearity of the system, moderate changes in freshwater input can induce transitions between different equilibrium states, leading to substantial changes in regional climate. As even local changes in freshwater flux are capable of triggering convective instability, quite small perturbations to the present hydrological cycle may lead to temperature changes of several degrees on timescales of only a few years.

THE North Atlantic Ocean today carries $(1.2 \pm 0.2) \times 10^{15}$ W of heat northwards[1,2]. Most of this heat transport is due to the vertical overturning cell associated with North Atlantic Deep Water (NADW) formation[3]; warm surface water flows northwards, sinks, and flows southwards as cold deep water. The volume transport of this 'conveyor belt' is about 17 ± 4 Sv (ref. 3; 1 sverdrup $= 10^6$ m^3 s^{-1}). This heating system makes the northern North Atlantic about 4 °C warmer than corresponding latitudes in the Pacific[4] and is responsible for the mild climate of Western Europe. Variations in NADW circulation therefore have the potential to cause significant climate change in the North Atlantic region.

Previous modelling studies have suggested that the NADW circulation is a nonlinear system which is highly sensitive to changes in freshwater forcing; it may collapse if a certain threshold is exceeded[5-9] and can show hysteresis behaviour[10,11]. There is mounting palaeoclimate evidence, particularly from sediment cores, showing that past climate shifts were associated with changes in NADW flow[12-15]. Recent coupled ocean–atmosphere model experiments investigating the effect of anthropogenic greenhouse gases on climate find that global warming would probably lead to reduced NADW formation[16,17].

Given the possibility of an anthropogenically triggered transition in NADW circulation, a systematic study of its sensitivity is urgently needed. Excessive computation costs make this not yet feasible using fully coupled ocean–atmosphere models. Here, a study of circulation transitions made with a global ocean circulation model coupled to a greatly simplified atmospheric model is presented. It is found that NADW circulation winds down when a bifurcation (first suggested by Stommel[5]) is passed, which the model predicts to occur when an additional freshwater input of less than 0.06 Sv is introduced into the catchment area of the North Atlantic. Convective instability can trigger a local shutdown of deep convection for even smaller regional changes in freshwater forcing, leading to rapid regional sea surface temperature (SST) changes within a few years. A transition to oscillatory behaviour[38] (a Hopf bifurcation) was also discovered, leading to a parameter range with self-sustained interdecadal oscillations.

Model and experiment design

The ocean model used in this study is the general circulation model (GCM) developed at the Geophysical Fluid Dynamics Laboratory (GFDL) in Princeton[18], in a coarse-resolution global configuration (Fig. 1*a*) with twelve vertical levels, similar to the models used in refs 17, 19 and 39. The model was driven by observed annual mean wind stress[20]. The surface flux of fresh water was derived from a spin-up experiment and prescribed as a fixed flux thereafter; this flux field is illustrated in ref. 21, where details of the model spin-up are also described. Regional integrals of the flux are shown in Fig. 1*b*; perturbations added to the freshwater flux for the sensitivity experiments are described below.

For thermal forcing, neither prescribing a fixed heat flux nor restoring the SST to prescribed values provides a realistic feedback response to large-scale ocean circulation changes[22]. Therefore, a simple atmospheric energy balance was used, which damps SST anomalies by horizontal diffusion of heat in the atmosphere and by longwave radiation. This approach is discussed in detail in refs 21 and 22. It reproduces the correct SST contrast between North Pacific and North Atlantic oceans in the model equilibrium as a result of oceanic heat transport, without prescribing it in the forcing. The damping of SST anomalies depends on their spatial scale; small anomalies are removed rapidly by atmospheric transport, and the largest scales damped only by longwave radiation to space. Scale selectivity is crucial for successfully modelling local heat loss in small convection regions at the same time as the large-scale response to oceanic heat transport.

With this surface forcing, the model reaches a steady equilibrium state after an integration time of ~5,000 years. This is used as a starting point for the experiments described below. In this state, the Atlantic thermohaline circulation has the familiar two-storey structure with a NADW overturning cell of 20 Sv stacked above an opposite turning cell of Antarctic Bottom Water of 7 Sv; the Pacific and Indian oceans derive their entire deep water from an inflow of 11 Sv from the south.

In the experiments reported here, slowly varying freshwater flux perturbations were added in different ocean regions (Fig. 1*a*). The perturbations were increased or decreased linearly in time, in order to trace the hysteresis response of the ocean circulation. The method was inspired by a study by Mikolajewicz and Maier-Reimer[11], who investigated the effect of thermal restoring boundary conditions on freshwater discharge events of 1,000–2,000 years duration. The aim of our study is different: we attempt to trace the equilibrium response of the NADW circulation to freshwater forcing changes, that is, to construct a bifurcation map and to identify critical transitions. Consequently, the forcing was varied at a much slower rate (up to 230 times slower than described in ref. 11). Freshwater flux is used as control variable for the experiments and is therefore specified. In reality there is a feedback of sea surface temperature on the freshwater flux[23], but recent work suggests this is only weak[24].

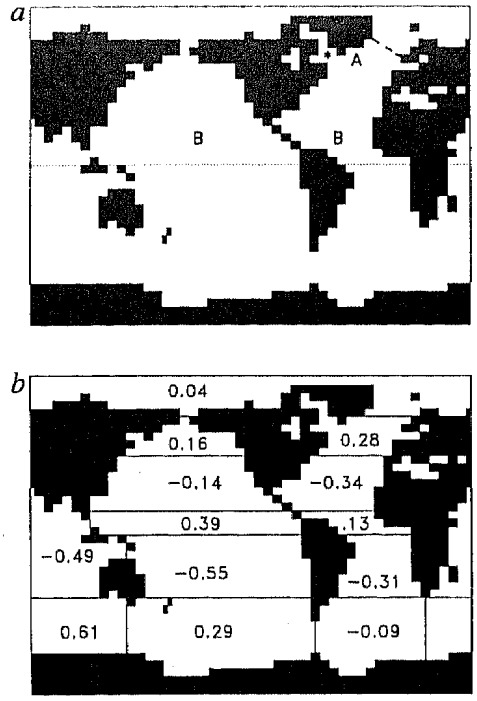

FIG. 1 *a*, Location map for the model experiments. The shaded areas A and B mark regions where freshwater forcing was varied; for region B the change was of opposite sign in the Atlantic and the Pacific. The Labrador Sea is marked with an asterisk, and the Greenland–Iceland–Scotland ridge separating the Atlantic from the Arctic is indicated as a dashed line. *b*, Regional integrals of net freshwater forcing in sverdrup (1 Sv = 10^6 m^3 s^{-1}). Positive values indicate net precipitation and occur in the intertropical convergence zone and in high latitudes; the subtropical gyre regions are characterized by net evaporation. The fluxes were obtained by forcing the ocean model towards observed surface salinity[4], and thus include the effect of river runoff. Note that there is no net volume transport and negligible net freshwater transport through Bering Strait in this model, so that oceanic transport across a given latitude in the Atlantic can be obtained by summing the surface fluxes from the Arctic; at the latitude of South Africa, the ocean circulation exports salt equivalent to a freshwater inflow of 0.2 Sv.

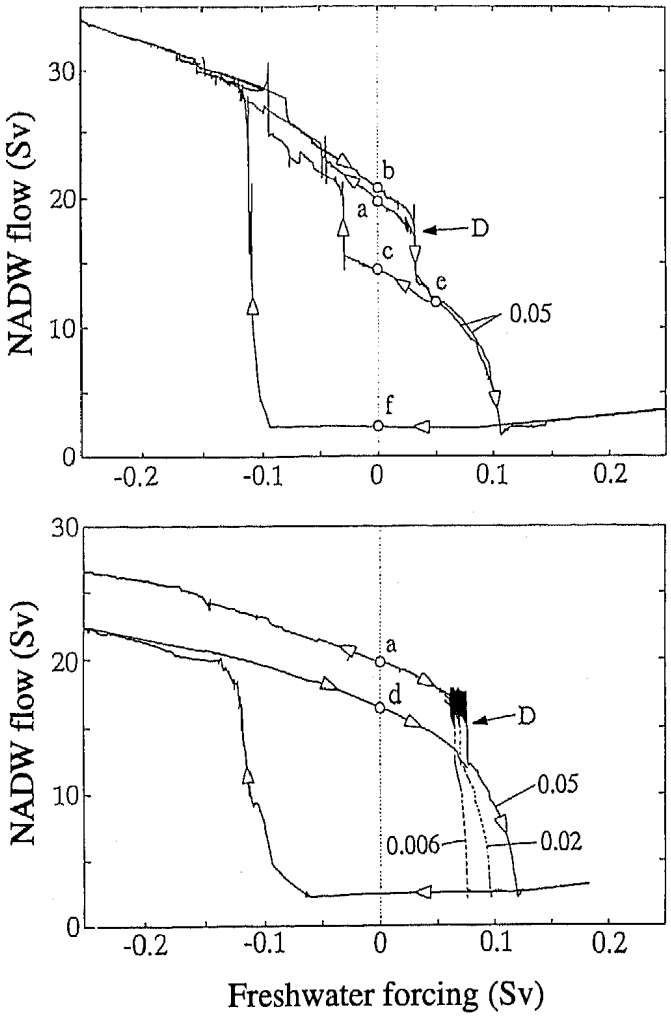

FIG. 2 Hysteresis response of the North Atlantic overturning circulation to a slowly changing freshwater forcing in the high latitudes (top panel) and the tropics (bottom panel; see Fig. 1 for exact locations). (NADW, North Atlantic Deep Water). Open circles mark true model equilibria obtained with constant freshwater forcing; the equilibrium marked a is the initial state at the start of the experiment. Arrows mark the direction in which the curve is traced. After one hysteresis loop, starting from a towards the right, the model arrives at equilibrium b. From there the right half of the hysteresis curve was traced a second time. Point c was reached by reversing at point e. Point f is an equilibrium with no NADW formation, under present-day forcing. The discontinuity D is the point where Labrador Sea convection ceases. In the lower panel, the right half of the hysteresis curve was traced at three different rates; the rate of freshwater forcing change is labelled in units of 10^{-3} Sv yr^{-1}.

Conveyor hysteresis

Figure 2 shows the NADW circulation (defined as the maximum of the meridional mass transport in the Atlantic, excluding the near-surface wind-driven layers) as a function of the freshwater perturbation for a number of experiments. In Fig. 2, top panel, fresh water was added to a region south of Greenland (labelled A on Fig. 1*a*), with the inflow increasing or decreasing by 0.05 Sv per 1,000 years; Fig. 2, bottom panel, shows experiments where fresh water was taken from the tropical Pacific and added to the tropical Atlantic (in the regions labelled B on Fig. 1*a*). Figure 2 bottom also includes two additional experiments where the forcing was changed at the slower rates of 0.006 and 0.02 Sv per 1,000 years. The initial state is labelled a.

The hysteresis curves show a decline in NADW overturning with increasing freshwater input into the North Atlantic. Beyond a certain value, overturning is essentially zero (the small remaining background transport is due to the fact that the meridional stream function never becomes negative everywhere, even in the absence of NADW formation). For an intermediate forcing range which includes present-day climate, NADW overturning can be either 'on' or 'off' (as in equilibrium f), depending only on initial conditions.

The inflow of Antarctic Bottom Water into the Atlantic decreases slightly as NADW flow weakens in the model. In the Pacific, the bottom water circulation also weakens, and after the breakdown of NADW flow an overturning cell of 10 Sv starts between 30° N and 60° N. This North Pacific cell (not shown) reaches 1,500 m depth and recirculates within the Northern Hemisphere with no outflow to the south, resembling the hemispheric circulation envisaged in Stommel's[5] original box model. It shows a clear hysteresis response even if the forcing changes only in the North Atlantic, constituting an interesting oceanic teleconnection between Atlantic and Pacific oceans.

Saddle-node bifurcation

The general shape of the hysteresis curves and their bimodal structure can be understood with the help of Stommel's[5] classical box model of the thermohaline circulation (which can be generalized to allow cross-hemispheric flow). Figure 3 shows the equilibrium solutions of this simple model as a function of freshwater flux. The positive branch corresponds to the overturning of NADW, while the negative flow branch corresponds to a reverse flow. The branch shown dashed is unconditionally unstable, and separates the basins of attraction of the two stable branches. Point S is a turning point, or saddle-node bifurcation, beyond which no stable positive solution exists. The thin lines were obtained by time integration with slowly increasing fresh-

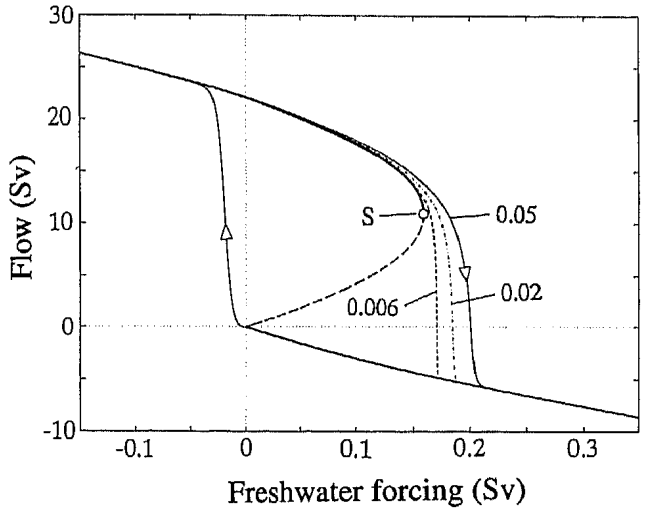

FIG. 3 Equilibrium flow and hysteresis response of Stommel's box model. Heavy curves show the analytical equilibrium solution; the dashed branch is unstable. S is the location of the saddle-node bifurcation. Thin lines are the result of a time integration with a freshwater forcing cycle identical to that used in the GCM experiments shown in Fig. 2. Note that freshwater forcing is given in absolute values for the box model, whereas for the GCM it is relative to the present-day climate.

water flux, as in the GCM experiments shown in Fig. 2. They show that the equilibrium branch can be tracked closely by a slow forcing increase—except near the bifurcation point, where the model response becomes infinitely sluggish.

A crucial question is where Stommel's bifurcation is located in the real world, and, as an approximation to this, in the GCM. In other words, what is the critical change in hydrological forcing which would trigger the shutdown of the present NADW conveyor belt circulation? From the box-model analogy, we conclude that the hysteresis experiments with the GCM can only provide an upper limit of this value. Figure 2, bottom panel, shows three GCM runs with different rates of forcing change (as in Fig. 3) and gives an upper limit of 0.075 Sv for the critical flux. To test for equilibrium, in a number of further experiments freshwater forcing was held constant after certain values had been reached. For the high-latitude perturbation (Fig. 2, top), the model was still stable and the hysteresis curve close to equilibrium at a flux of 0.05 Sv, but at 0.06 Sv it was beyond the bifurcation and wound down. Similarly, for the low-latitude perturbation the bifurcation was found to be between 0.056 and 0.062 Sv. The corresponding critical rate of NADW overturning is close to 12 Sv; smaller rates of NADW formation cannot apparently be sustained by the model.

It is remarkable that the critical amount of freshwater input is essentially the same, whether added in the high-latitude convection region or in the low latitudes. This is because the mechanism underlying Stommel's bifurcation is a large-scale advective mechanism. It does not much matter where the fresh water is added, as long as it passes through the NADW loop before leaving the Atlantic, that is, it is added to the "NADW catchment area". This catchment area will not have a sharp boundary in a turbulent ocean; for example, fresh water added to the South Atlantic can be expected partly to flow north in the conveyor and partly to exit to the Southern Ocean through wind-driven circulation. The catchment area also depends on the circulation itself.

It is difficult to assess which changes in atmospheric circulation would be required to increase the freshwater transport into the NADW catchment area by 0.06 Sv, but Fig. 1*b* indicates that the change would only be a fraction of the climatological flux. In the coupled experiment of Manabe and Stouffer[17,25] for a quadrupling of the atmospheric level of CO_2, NADW formation is completely extinguished by a net precipitation increase in the North Atlantic, while sea-ice melting makes a negligible contribution. If a freshwater flux of 0.06 Sv were to be obtained only by melting sea ice, the entire Arctic sea-ice volume ($2–3 \times 10^{13}$ m^3) would need to melt during a period of 10–15 years, a time span too short to cause an advective spin-down of the circulation. The timescale of the shutdown is determined by the advection of salt in the overturning circulation and is typically several hundred years; the more the critical flux is exceeded, the faster the spin-down. Sea-ice melting is, therefore, not a viable mechanism for causing an advective spin-down, but could lead to convective transitions as discussed in the next section. For comparison, meltwater inflow from the disintegration of continental ice sheets at the end of the last glacial peaked at 0.44 Sv and lasted many centuries[26].

Convective instability

Although the overall shape of the hysteresis curves can be explained by Stommel's box model, there are also interesting discontinuities, most notably the one marked D in Fig. 2. When we start from point e on the equilibrium curve and move to the left, a new equilibrium branch is found with a lesser NADW overturning rate. And when a full hysteresis cycle is completed, we arrive at not the initial state a, but a different equilibrium state (b or d respectively). We are thus finding multiple equilibrium states with different NADW formation rates under the same forcing.

Similar multiple equilibria have previously been found and analysed in idealized models[27–29]; they are linked to different stable convection patterns and are caused by a positive feedback mechanism which can make convection self-sustaining once it has been established at a certain point. The convection patterns for several equilibria marked in Fig. 2 are shown in Fig. 4. The crucial difference between model states with ~20 Sv overturning and those with only ~16 Sv overturning is the absence of Labrador Sea convection in the latter. Time series of convection depth at single points (not shown) confirm that at the discontinuity D Labrador convection shuts down. Other small jumps in the circulation time series can generally be attributed to a change in convection somewhere in the model. Associated circulation changes appear almost instantaneous, as adjustment to convection changes occurs through a mechanism of wave propagation[30,31] which takes only a few years to complete. Convective instability is therefore a mechanism that could lead to rapid climate shifts such as the Younger Dryas event[29].

Convective instability does not depend on the large-scale freshwater budget but on local flux. This is why the shutdown of Labrador convection occurs for a much smaller freshwater input for the high-latitude perturbation than for the low-latitude perturbation (compare Fig 2 top and bottom). Further experiments showed that a perturbation of 0.015 Sv is enough to cause the shutdown if targeted directly at the Labrador Sea. This demonstrates that rather small changes in freshwater forcing may lead to regional shutdown of convection. In the real world and in fully coupled models, the distinction between similar equilibria (such as a and b) may be blurred by atmospheric variability, but qualitatively different convection patterns (such as a and c) should represent distinct climate states (see the discussion in Rahmstorf[21]). Sediment-core results[15] have linked past climate change to a regional shift in NADW convection, from the Norwegian Sea to a location south of Iceland.

Interdecadal oscillations

A further interesting feature of the hysteresis curves is the occurrence of interdecadal oscillations in certain parameter ranges. The most spectacular oscillation arises in Fig. 2, bottom panel, just before the Labrador discontinuity D. Figure 5 shows a close-up view of the relevant section of the curve; it reveals that a Hopf bifurcation (H) leads to a transition from a stable model solution to a limit cycle with a period of 22 years. This period is independent of the rate at which freshwater input is increased.

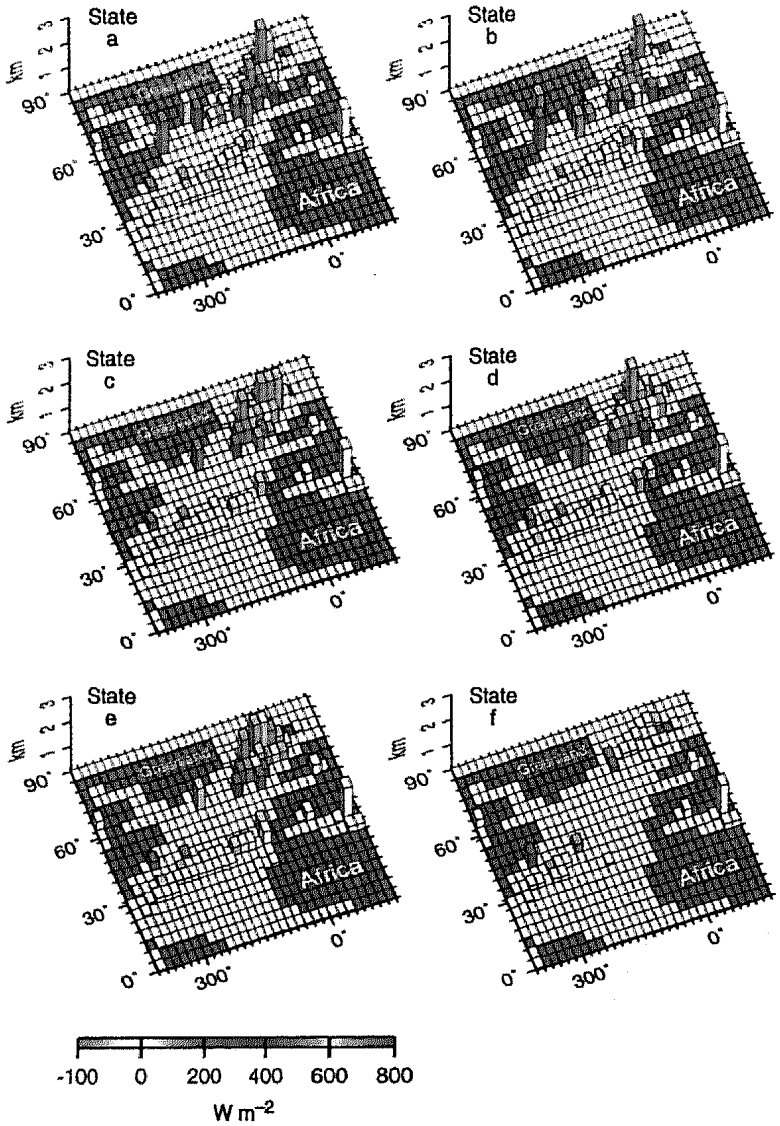

FIG. 4 Convection patterns in the North Atlantic for six equilibrium solutions (states a–f) of the ocean model as labelled in Fig. 2. The height of the columns shows convection depth from the surface, and colour indicates the amount of heat (W m^{-2}) brought to the surface by convection. Convection is the main process by which the heat brought to the north in the conveyor circulation is released from the water column. Note that states a and b have convection in the Labrador Sea, whereas in c–e NADW is formed only east of Greenland. State f is a 'southern sinking' state without NADW formation.

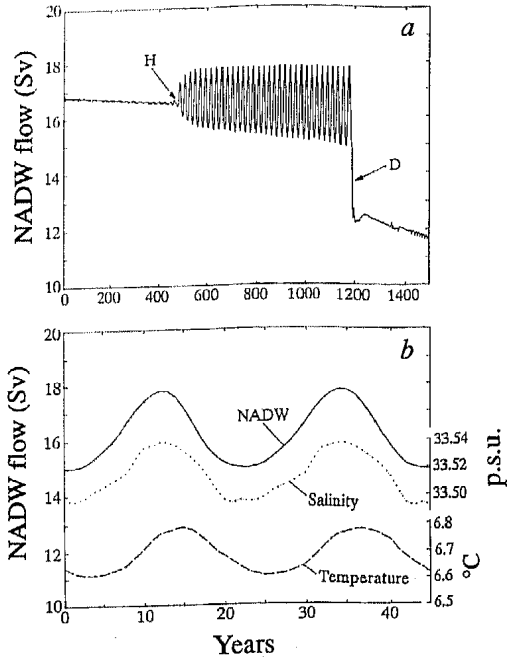

FIG. 5 *a*, Close-up view of the oscillations visible in Fig. 2, bottom panel, just before the shut-down point D of Labrador convection. The time axis is labelled in years with an arbitrary origin. At point H, the model passes a Hopf bifurcation, where the stable equilibrium state gives way to a limit cycle with a period of 22 years. Note that the amplitude initially increases as the square root of the control parameter (freshwater flux, which in this case is proportional to time); a characteristic feature of Hopf bifurcations[38]. *b*, Two periods of the oscillation at higher time resolution. Also shown are surface salinity and temperature, averaged over the Atlantic north of 50° N.

The overturning rate varies by as much as 3 Sv, and the average temperature of the high-latitude North Atlantic by 0.2 °C. The temperature maximum lags behind the overturning maximum by about 3 years. As one would expect from the short period, this oscillation is local to the North Atlantic; it is also deep—the flow oscillates in a region between 20° N and 60° N over the whole depth range. Surprisingly, Labrador Sea convection is not affected; convection depths remain completely stationary throughout the oscillation. The sea surface temperature pattern associated with the oscillation is shown in Fig. 6*a*. With its maximum near Newfoundland, it resembles the observed interdecadal variability pattern shown by Kushnir[32], except that it lacks the second maximum found in the data near the sea-ice margin north of Iceland. This second maximum may be linked to sea-ice variations; no ice model is included in the present study. A much weaker oscillation with a period of 16 years arises in the high-latitude experiment (Fig. 2, top), again just before the Labrador convection shuts down. Similar interdecadal SST oscillations centred on the Labrador region have been found in a number of studies with different models[33–35].

Consequences for climate

Given the large heat transport of the NADW conveyor belt, it is natural to ask what the bifurcations described above mean for Atlantic surface temperatures. Because of the simpleatmospheric heat budget employed, the model has a limited capacity to predict SST changes resulting from circulation changes. The equilibrium with the strongest overturning (state b), also has the warmest high-latitude SST. Figure 6 shows SST differences of other model states compared to initial state a, as well as the SST change over one of the oscillation cycles discussed above (Fig. 6*a*). The interdecadal oscillation has a range of 0.7 °C near Newfoundland and decreases to under 0.2 °C near the European coast. The difference between normal and weak NADW circulation equilibria (Fig. 6*b*) is larger; it reaches a maximum of 2.5 °C near Newfoundland. The cooling predicted for a total shutdown of NADW circulation (Fig. 6*c*) reaches a maximum of 6 °C near Greenland, with widespread cooling of over 4 °C across the Atlantic. Note that a fully coupled experiment would probably show an amplified temperature response near ice margins due to the ice–albedo feedback (not included in this model). The cooling effect would also extend further north in a model that produces more NADW north of the Greenland–Scotland ridge.

Overall features of the bifurcation map

The experiments discussed in this Article provide a map of the equilibrium states and bifurcation points of the Atlantic thermohaline circulation in a global ocean GCM, as a function of the surface freshwater flux. The central feature is a saddle-node bifurcation first described by Stommel[5] in 1961; it is the point beyond which the NADW circulation cannot be sustained, wind-

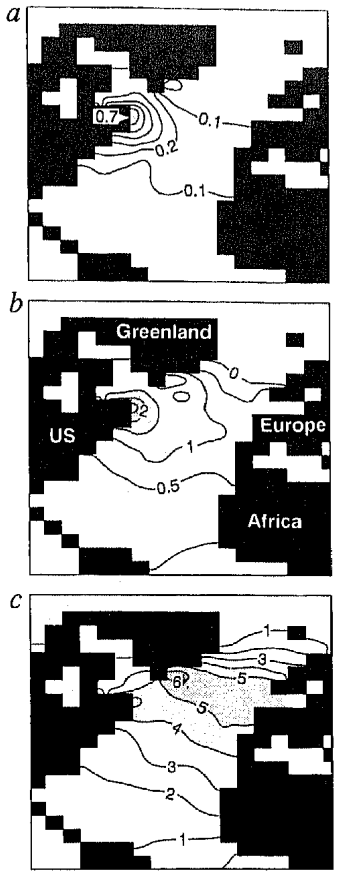

FIG. 6 Sea surface temperature change (in °C) for three types of NADW circulation changes. *a*, Difference between warm and cold phase of the inter-decadal oscillation; *b*, difference between 'normal' and 'weak' NADW equilibria (states a minus c of Fig. 2); *c*, difference between 'normal' and absent NADW circulation (states a minus f of Fig. 2). Shading highlights regions of strongest sea surface temperature change; states with stronger NADW overturning are warmer in each case.

ing down on an advective timescale of centuries. The spin-down is characterized by gradually weakening heat transport and convection, and must be distinguished from the dramatic instability which occurs when convection is suddenly interrupted in the entire North Atlantic—a much faster process known as 'polar halocline catastrophe'. Due to the slow forcing change this kind of collapse, which may be temporary or permanent, was not observed in the experiments reported here, but it has been found in models subjected to rapid and massive meltwater discharge[9,22,39].

Stommel's bifurcation is a very robust feature, found in models of different complexity—from simple box models to GCMs. In our GCM, the critical point is reached for an additional freshwater input of only 0.06 Sv into the NADW catchment area. This is much less than a previous estimate of 0.3 Sv, which was obtained with an idealized two-dimensional model without wind forcing[10]. The new estimate is an uncomfortably small perturbation to the present hydrological cycle (compare Fig. 1*b*). It is impossible to give an error margin on this estimate, but it depends not on regional details, only on the basin-scale circulation, which the model reproduces quite well. A slow spin-down, which seems to be of the type discussed here, was found in a coupled model scenario[17] for a quadrupling of atmospheric CO_2.

A second feature of the bifurcation map is the existence of multiple states with different rates of NADW formation. Transitions between these states can be triggered for even smaller, regional changes in the freshwater budget, and they can lead to substantial SST changes within a few years. In this model, the major transition is between states with and without convection in the Labrador Sea. This result, however, depends on regional details of convection, which are not properly resolved in a coarse model; the physical principle is likely to be robust, although the specific details may not be. In the real world, a substantial part of NADW is formed north of Iceland, but present climate models have trouble representing the physics of the overflow over the Greenland–Scotland ridge. There is good evidence that convection north of Iceland shut down in glacial times[15]. It is possible that this convection region is more vulnerable to climate change than the one in the Labrador Sea; this cannot be determined using the present model. The freshwater balance of this convection region can be upset by precipitation changes, by melting ice (melting Arctic sea ice at a rate of 5 cm yr^{-1} would provide a freshwater flux of ~0.01 Sv), but also by changes in regional currents. For example, the East Greenland current presently removes some of the net precipitation falling over the Arctic seas, transporting it southwards over the sill[36]. It is therefore difficult to establish how vulnerable the present convection pattern is to climate changes, or indeed whether deep convection north of Iceland has ceased already[37].

The third feature is the existence of the Hopf bifurcation, leading to an oscillation of the meridional overturning rate centred on the Labrador region. This bifurcation suggests that there are parameter ranges where the ocean circulation is intrinsically steady and would vary only in response to variable atmospheric forcing, and other parameter regions where the ocean generates self-sustained interdecadal oscillations. This opens the possibility that a change in hydrological forcing can shift the North Atlantic from a stable climate to an oscillatory regime, or vice versa. It will be an important topic of future research to establish the exact forcing conditions under which oscillations occur. □

Received 7 July; accepted 13 October 1995.

1. Hall, M. M. & Bryden, H. L. *Deep-Sea Res.* **29,** 339–359 (1982).
2. Rintoul, S. R. & Wunsch, C. *Deep-Sea Res.* **38,** S355–S377 (1991).
3. Roemmich, D. H. & Wunsch, C. *Deep-Sea Res.* **32,** 619–664 (1985).
4. Levitus, S. *Climatological Atlas of the World Ocean* (US Dept of Commerce, NOAA, Washington DC, 1982).
5. Stommel, H. *Tellus* **13,** 224–230 (1961).
6. Bryan, F. *Nature* **323,** 301–304 (1986).
7. Manabe, S. & Stouffer, R. J. *J. Clim.* **1,** 841–866 (1988).
8. Marotzke, J. & Willebrand, J. *J. phys. Oceanogr.* **21,** 1372–1385 (1991).
9. Maier-Reimer, E. & Mikolajewicz, U. in *Oceanography* (eds Ayala-Castañares, A., Wooster, W. & Yáñez-Arancibia, A.) 87–100 (UNAM, Mexico, 1989).
10. Stocker, T. F. & Wright, D. G. *Nature* **351,** 729–732 (1991).
11. Mikolajewicz, U. & Maier-Reimer, E. *J. geophys. Res.* **99,** 22633–22644 (1994).
12. Broecker, W. S., Peteet, D. M. & Rind, D. *Nature* **315,** 21–26 (1985).
13. Boyle, E. A. & Keigwin, L. *Nature* **330,** 35–40 (1987).
14. Keigwin, L. D., Curry, W. B., Lehman, S. J. & Johnson, S. *Nature* **371,** 323–326 (1994).
15. Sarnthein, M. *et al. Paleoceanography* **9,** 209–267 (1994).
16. Cubasch, U. *et al. Clim. Dyn.* **8,** 55–69 (1992).
17. Manabe, S. & Stouffer, R. J. *Nature* **364,** 215–218 (1993).
18. Pacanowski, R., Dixon, K. & Rosati, A. *The GFDL Modular Ocean Model Users Guide* (Tech. Rep. Vol. 2, Geophysical Fluid Dynamics Laboratory ocean group, Princeton, 1991).
19. England, M. H. *J. phys. Oceanogr.* **23,** 1523–1552 (1993).
20. Hellerman, S. & Rosenstein, M. *J. phys. Oceanogr.* **13,** 1093–1104 (1983).
21. Rahmstorf, S. *Clim. Dyn.* **11,** 447–458 (1995).
22. Rahmstorf, S. & Willebrand, J. *J. phys. Oceanogr.* **25,** 787–805 (1995).
23. Marotzke, J. in *Ocean Processes in Climate Dynamics: Global and Mediterranean Examples* (eds Malanotte-Rizzoli, P. & Robinson, A. R.) 79–109 (Kluwer, Dordrecht, 1994).
24. Hughes, T. M. C. & Weaver, A. J. *J. phys. Oceanogr.* (in the press).
25. Manabe, S. & Stouffer, R. J. *J. Clim.* **7,** 5–23 (1994).
26. Fairbanks, R. G. *Nature* **342,** 637–642 (1989).
27. Lenderink, G. & Haarsma, R. J. *J. phys. Oceanogr.* **24,** 1480–1493 (1994).
28. Rahmstorf, S. *J. Clim.* (in the press).
29. Rahmstorf, S. *Nature* **372,** 82–85 (1994).
30. Kawase, M. *J. phys. Oceanogr.* **17,** 2294–2316 (1987).
31. Döscher, R., Böning, C. W. & Herrmann, P. *J. phys. Oceanogr.* **24,** 2306–2320 (1994).
32. Kushnir, Y. *J. Clim.* **7,** 142–157 (1994).
33. Delworth, T., Manabe, S. & Stouffer, R. J. *J. Clim.* **6,** 1993–2011 (1993).
34. Weaver, A. J., Aura, S. M. & Myers, P. G. *J. geophys. Res.* **99,** 12423–12442 (1994).
35. Weisse, R., Mikolajewicz, U. & Maier-Reimer, E. *J. geophys. Res.* **99,** 12411–12421 (1994).
36. Stigebrandt, A. *Palaeogeogr. Palaeoclimatol. Palaeoecol.* **50,** 303–321 (1985).
37. Schlosser, P. *et al. Science* **251,** 1054–1056 (1991).
38. Drazin, P. G. *Nonlinear Systems* (Cambridge Univ. Press, 1992).
39. Manabe, S. & Stouffer, R. J. *Nature* **378,** 165–167 (1995).

ACKNOWLEDGEMENTS. I thank J. Willebrand for supporting my work, M. England for sharing his model code, and D. Smart for editing the manuscript. This work was funded by the German Research Ministry; computations were performed at the German Climate Computer Centre in Hamburg.